

Validation and testing of a sea-level cosmic ray event generator

8203X

Supervisor: Dr. Christopher Lester

Except where specific reference is made to the work of others, this work is original and has not been already submitted either wholly or in part to satisfy any degree requirement at this or any other university.

Abstract

A cosmic ray event generator create by a previous student[1] was tested and necessary corrections were made to the generator. Significant changes were made to the generator's 'all angles' generation mode using the theoretical model presented in [2]. The generator's output has been tested up to 20TeV in the case of vertical muons and up to a maximum zenith angle of 80° for the 'all angles' mode. The generator is also able to recreate a $\cos^n\theta$ spectrum at low energies and a $\sec^n\theta$ spectrum at high energies.

1 Introduction

Muon tomography is a subject of interest in recent years for its potential applications in imaging large structures for cracks and defects. This technique has already been used to image various structures of interest, such as a railway tunnel in the UK [3], a nuclear reactor following a tsunami[4] and most famously, the Egyptian pyramids[5]. This project aims to improve such imaging techniques by focusing on creating a cosmic ray event generator which produces a more realistic energy and angular spectrum. In particular, access to a reliable estimate of near-horizontal muons, a part of the muon spectrum which is not very well documented, could help improve the resolution of images produced by muon tomography techniques.

The generator was originally created by a previous student, as described in [1]. As part of this project, the output of the generator was tested and corrections have been made to the generator. A majority of the work was focused on creating an accurate angular spectrum and significant changes to the functionality of the generator were made.

1.1 Conventions

Throughout this paper, the angle θ refers to the zenith angle of an incoming muon defined to be the angle as measured against the vertical axis. The muon flux is also assumed to be invariant under rotations in the azimuthal angle such that the trajectory of the muon is completely specified by an energy and zenith angle.

Energy is measured in GeV , area in m^2 and time in s . The differential flux is measured in $\text{s}^{-1}\text{Sr}^{-1}\text{m}^{-2}\text{GeV}^{-1}$ or marked as (relative) where scaling has been applied.

2 Theoretical background

2.1 Modelling the differential muon flux

As part of the generation method, a theoretical model of the muon flux is required. This model is used to generate vertical muons at high energy and to obtain an expected angular distribution for non-vertical muons.

Following the analysis performed in [2], the differential muon flux is given by

$$\frac{dN}{dE} \approx S_\mu \frac{0.14E_\mu^{-2.7}}{\text{cm}^2\text{sSrGeV}} \left\{ \frac{1}{1 + \frac{1.11E_\mu \cos(\theta)}{115\text{GeV}}} + \frac{0.054}{1 + \frac{1.11E_\mu \cos(\theta)}{850\text{GeV}}} \right\} \quad (1)$$

where E_μ is the muon energy, θ is the zenith angle and S_μ is the suppression factor given by

$$S_\mu = \int_0^{X_0 \cos \theta} \frac{dX}{\Lambda_N} \left(\frac{X \cos \theta}{X_0} \right)^{p_1} \left(\frac{E_\mu}{E_\mu + \alpha \left(\frac{X_0}{\cos \theta} - X \right)} \right)^{p_1 + \gamma + 1} \exp \left(- \frac{X}{\Lambda_N} \right) \quad (2)$$

which reduces to

$$S_\mu \approx \left(\frac{\Lambda_N \cos \theta}{X_0} \right)^{p_1} \left(\frac{E_\mu}{E_\mu + \frac{2GeV}{\cos \theta}} \right)^{p_1 + \gamma + 1} \Gamma(p_1 + 1) \quad (3)$$

in the limit of infinite observation depth, $X_0 \rightarrow \infty$. The values Λ_N and γ are the characteristic decay length and power index for a given power law spectrum describing the initial muon flux. X is the slant depth, α is the rate of energy loss and p_1 is given by $\epsilon_\mu / (E_\mu \cos \theta + \alpha X_0)$ where ϵ_μ is the energy of the parent. In equation 1, the two terms represent the two main production channels for atmospheric muons, $k^\pm \rightarrow \mu^\pm + \nu_\mu(\bar{\nu}_\mu)$ and $\pi^\pm \rightarrow \mu^\pm + \nu_\mu(\bar{\nu}_\mu)$. The charged pions and kaons are produced by collisions of high energy nuclei (primarily hydrogen and helium nuclei) which then interact further to form secondary cosmic rays. The suppression factor represents the probability that a muon will survive travelling to the surface. The numerical values in equation 1 are all fitted to experimental values.

The assumption of infinite observation depth is valid for cosmic ray muons which are expected to be produced at an altitude of $\sim 15km$ [6] which is much larger than other length scales.

2.2 Angular muon spectrum

It is generally cited that the angular muon flux should obey a $\cos^n \theta$ relation where n is ~ 2 [7]. This distribution was used by the previous student to produce an angular distribution for the generator. However, the actual value of n seems to be very dependent on the minimum cutoff energy of the muons. It is suggested in [6] that muons with energy $\sim 3GeV$ follow this $\cos^2 \theta$ distribution and that this distribution approaches a $\sec \theta$ distribution for high energies. Other works have measured the exponent to be anywhere from $\sim 1.7 - 2.3$ depending on the energy cutoff and various environmental factors[8][9]. For higher energies, experimental data on the angular spectrum of muons is very sparse.

Looking to improve on the accuracy of the generator's accuracy, attempts were made to characterize the exponent n based on the energy of the muon. However, no consistent relationship was found between these two quantities so an alternative method was used to generate the angular muon spectrum. The implementation of this is discussed in section 4.2.

2.3 Environmental effects

There are several experiments which attempt to observe the effects of environmental factors on the sea-level muon flux. The effects of seasonal variations at various geographical locations on the muon flux are measured in [10]. The magnitudes of these shifts in muon flux was around 4% when considering the pressure corrected fluxes (see figure 1 in [10]) with a period of one year.

For the purposes of this generator, these environmental factors are ignored. The inclusion of these factors require a very long time to implement for a relatively small improvement in accuracy.

3 Validation of the generator

The generator uses a rejection sampling algorithm[11] to generate the momenta and zenith angles for muons. The differential flux is used as a probability distribution for the rejection sampling. It runs in two modes, one which generates only vertical muons and one which generates muons at all zenith angles. This section summarizes tests done on the generator before any changes have been made from the generator described in [1].

3.1 Vertical muon generation

The previous student reported inconsistencies in the data set that they obtained, claiming that the data measured by the BESS spectrometer[12] was systematically lower than other data sets as shown in figure 1. A best fit line was obtained by fitting the rest of the data to an order 3 polynomial.

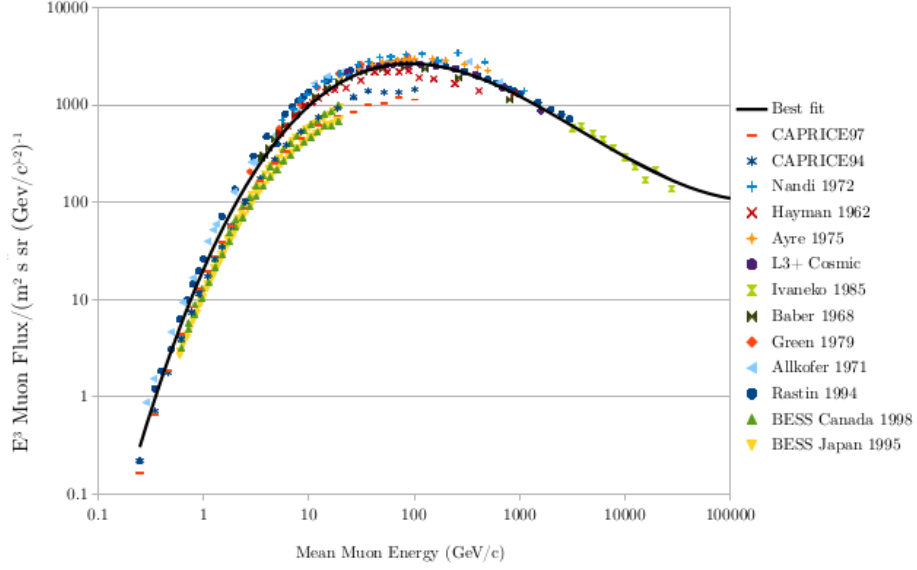


Figure 1: A plot of the best fit curve used to generate the vertical muon spectrum compared to the experimental data. The BESS data set is seen to be systematically lower than other data sets and was not included in the fit. However, later testing proved that this curve is compatible with the BESS data set as well. This plot was taken from the paper written by the previous student working on the project[1].

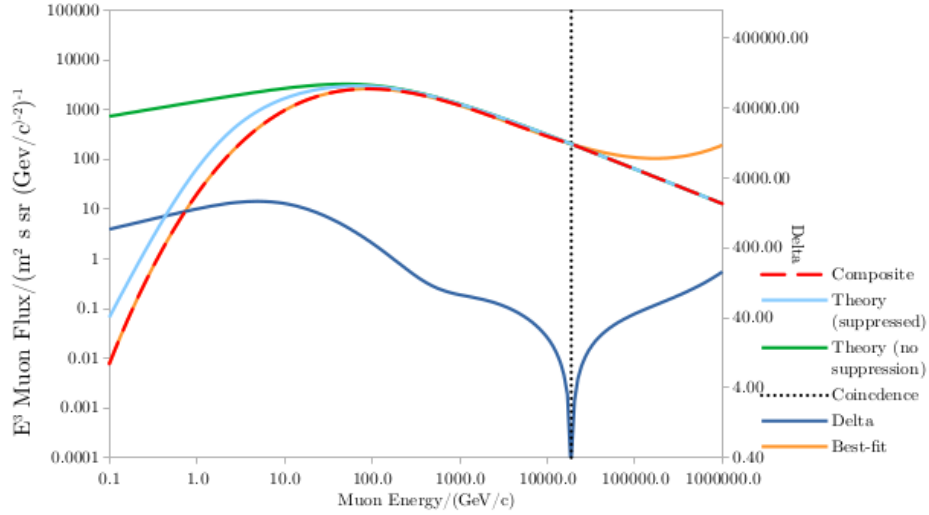


Figure 2: A plot showing 'composite', the curve used to generate vertical muons in comparison to other relevant curves. For energies below the cutoff point, the curve is the best fit line from figure 1. Above this cutoff, the curve is the theoretical model from equation 1.

In order to verify this curve, data measured by Tsuji et al.[13] was compared to the best fit curve as this data set was not included in the original fit. The excluded BESS dataset was also used as part of this test. The source of the lower differential flux was identified to be the difference in normalization values used by each experiment. These values differ depending on the date of the experiment as measurements of the absolute muon flux change with improvements in experimental methods. For example, the value used in [14] was noted to be 26% higher than the values used by previous experiments.

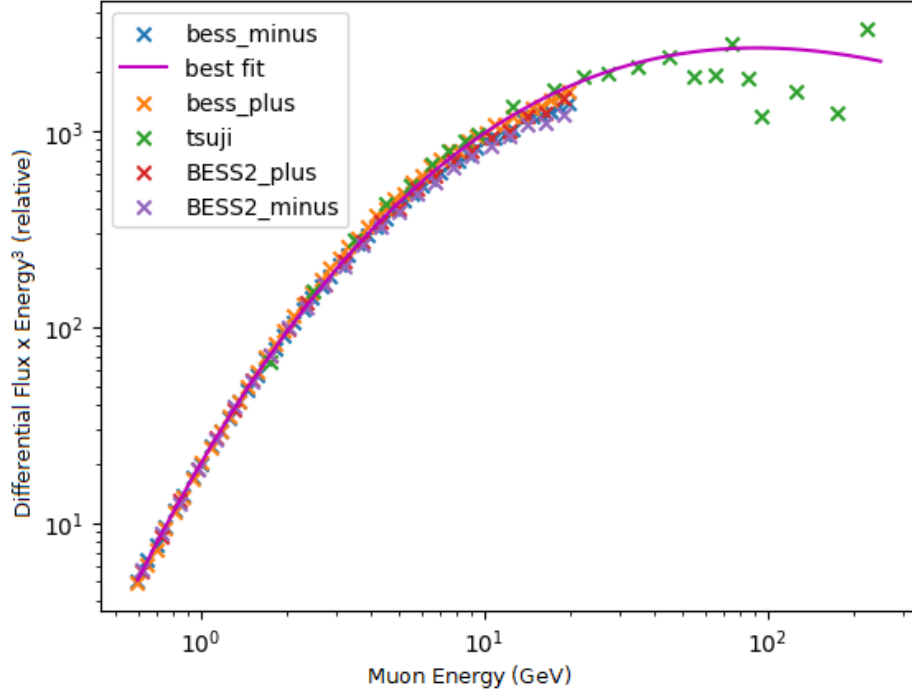


Figure 3: A plot of the best fit curve and experimental data collected by the BESS spectrometer [12] and Tsuji et al [13]. The two experimental data sets have been re-scaled such that they have the same total flux as the best fit line. Plus and minus for the BESS data set refers to positive and negative muons with 'bess' being data measured in Tsukuba, Japan and 'BESS2' referring to data measured in Lynn Lake, Canada. Following the scaling, both data sets now agree with the best fit line from figure 1.

Fortunately, the different normalizations are not a problem for the rejection sampling algorithm. Since the differential flux is used as a probability distribution, the generator is invariant to scaling. This effectively means that only the shape of the curve matters, not the absolute value of the curve. Allowing for scaling, the best fit curve now shows remarkable agreement with the initially excluded values measured by the BESS spectrometer and the Tsuji et al. data. As a result, generation using the best fit curve should accurately reproduce the vertical muon spectrum. The curve used to generate muons is shown in figure 2.

3.2 Generator output - Vertical muons

The generator was set to generate 200000 particles using both of the generator settings. For the 'vertical only' setting, the differential flux of the best fit line was compared with the generator output by binning the generator output and estimating a differential flux from the binned results. The results were binned by taking the log of the energy of each particle and putting them into bins of size 0.1 with the sizes adjusted so that the minimum number of particles in any bin is five.

For the 'all angles' setting, muons with zenith angle less than 2.5° were selected and binned in the same way as the muons generated by the 'vertical only' setting. The 2.5° acceptance angle was chosen to reflect typical experimental setups in this field which uses bin width ranging anywhere from $1 - 5^\circ$ [15][16]. The results are shown in figure 4.

The generator output shown does not match the best fit line in either case. For the 'vertical only' mode, the solution was a small bug fix and did not require any significant changes to the functionality of the generator. The results after applying the fix do appear to match up very well for the 'vertical only' mode. However, this was not true for the 'all angles' mode. Since the energy spectrum for all angles is based on the theoretical model (equation 1), it does not match up for low energies as suggested by figure 2. This was considered a very big problem for the generator since it is not self-consistent. Significant changes had to be made to the generation methods of the generator in order to correct this. Corrections are described in detail in section 4.2, with the final results presented throughout section 5.

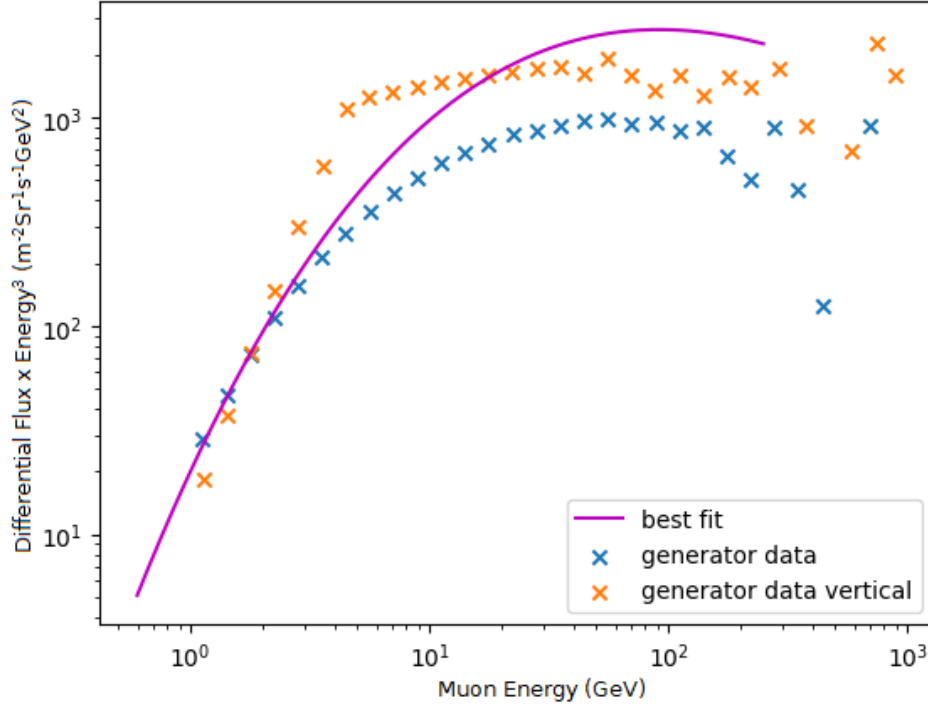
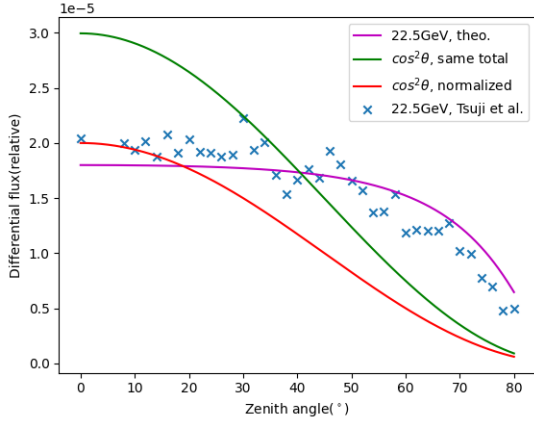


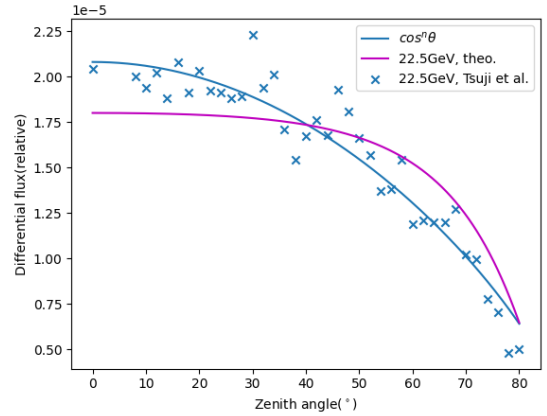
Figure 4: A plot of the estimated differential flux against the energy of the two generator output modes before any changes were made. 'Generator data vertical' shows the output generated by the generator's 'vertical only' mode. 'Generator data' shows the output of the 'all angles' mode.

3.3 Non-vertical muons

The $\cos^2\theta$ relationship was tested against data collected in [13]. This data set was chosen because it covers a large range of zenith angles and has the angular spectrum at relatively high energies (12.5, 22.5 and 45.0 GeV). The result of the attempts to fit the data is shown in figure 5.



(a) $\cos^2\theta$ and equation 1.



(b) $\cos^n\theta$ and equation 1.

Figure 5: Two plots showing possible fits of data in [13]. The $\cos^2\theta$ distribution does not accurately describe the muon angular spectrum at this energy. A least squares fit of the $\cos^n\theta$ curve gives a value of $n = 0.673$. This shows the very wide range of exponents depending on the energy cutoff.

The $\cos^2\theta$ relationship seems to be a very poor fit for the angular spectrum for this energy range. Several methods of scaling the $\cos^2\theta$ distribution were attempted including normalizing so that the total flux is the same, performing a least squares fit and fitting so that the values agreed at 0° . However, none of these methods produced a curve which was deemed suitable to describe the experimental data. This is not unexpected as most experiments done on the subject put the energy cutoff for muons very low

(generally around the $0.1 - 5\text{GeV}$ range). However, it appears that the angular spectrum predicted in equation 1 still works well around this energy range. Additionally, it is possible to find a $\cos^n\theta$ curve that works well for this energy by performing a least square fit on the experimental data. The value of n , in this case is $n = 0.673$. Since the value of n fluctuates significantly with energy, using a $\cos^n\theta$ curve would require a much larger amount of experimental data than is currently available in order to estimate n for all energies. To quantify these results, a linear regression test was done on both the $\cos^2\theta$ relationship and the one predicted in equation 1. The resulting fit had R^2 values of 0.901 and 0.946 respectively. Thus, it was decided to assume that the angular spectrum predicted in the theoretical model was correct and this result was used in subsequent fixes to the generator.

3.4 Generator output - Non-vertical muons

Despite the $\cos^2\theta$ relationship not matching the energy distribution very well at high energies, it is expected that the overall energy spectrum should still be reasonably accurate as the majority of muons at sea level have very low energies. However, the generator allows users to set a lower limit to the energy range. It was found that if this energy range was set to any value more than $3 - 4\text{GeV}$, the generator can no longer produce a reasonable estimate of the angular spectrum. As an example, the generator was set to produce 20000 muons with a lower limit of 20GeV to match the energy range given in [13]. The comparison of the generator output and the experimental data above is shown in figure 6.

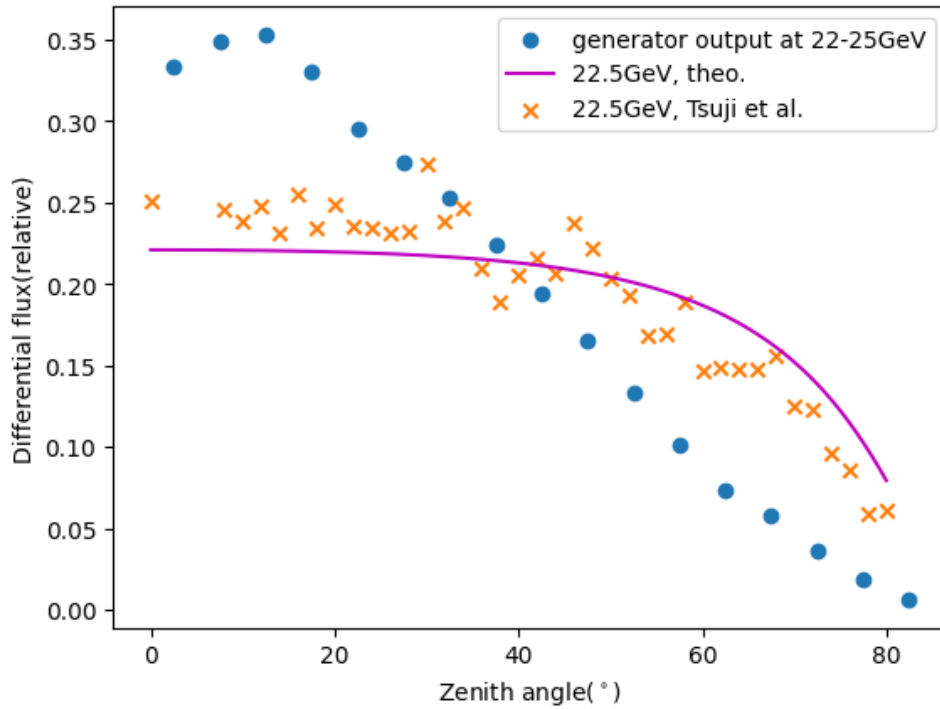


Figure 6: A plot of the generator output compared to experimental data in [13]. To generate this plot, the generator was set to produce muons between $22 - 25\text{GeV}$ and a differential flux was estimated from the data. The flux has been scaled to ensure the same total flux as the experimental data.

Following this, more tests were done to make sure that the rejection sampling algorithm does accurately reproduce the curve used as the probability distribution for the rejection sampler.

The generator was set to generate 20000 muons using the 'all angles' setting. Following the typical bin sizes found in experiments[16], the muons were binned with a bin width of 5° and the appropriate scaling was applied and compared to the expected $\cos^2\theta$ distribution (figure 7).

It was found that the generator was accurately reproducing the given curve using the 'all angles' setting. The result after initial bug fixes is shown in figure 8.

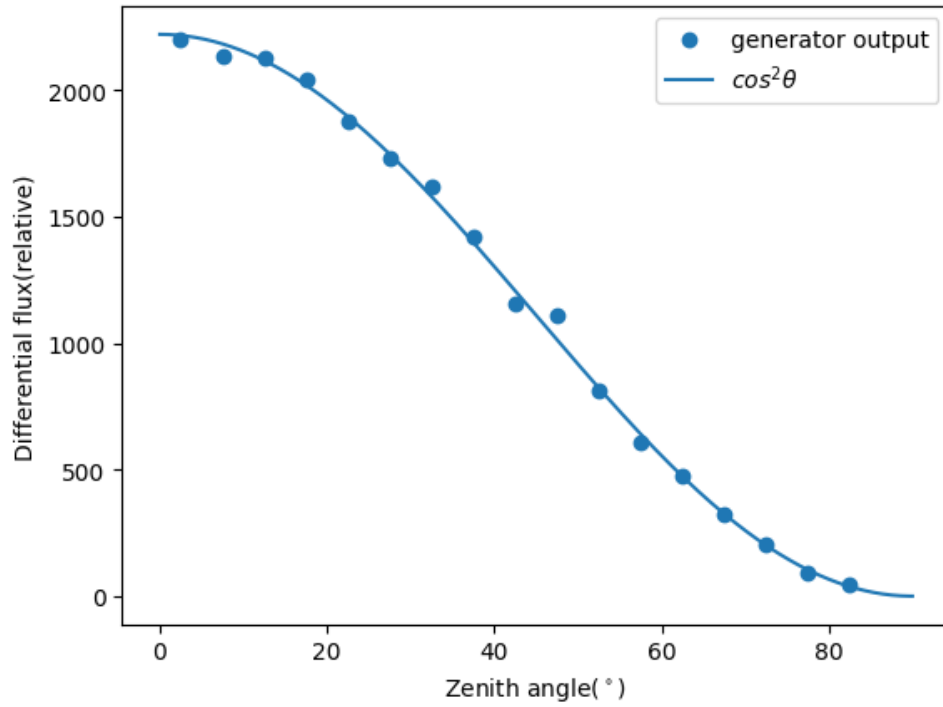


Figure 7: A plot of the generator output compared to the expected $\cos^2\theta$ distribution. This was done to make sure that the rejection sampling algorithm implemented by the previous student produced the expected results.

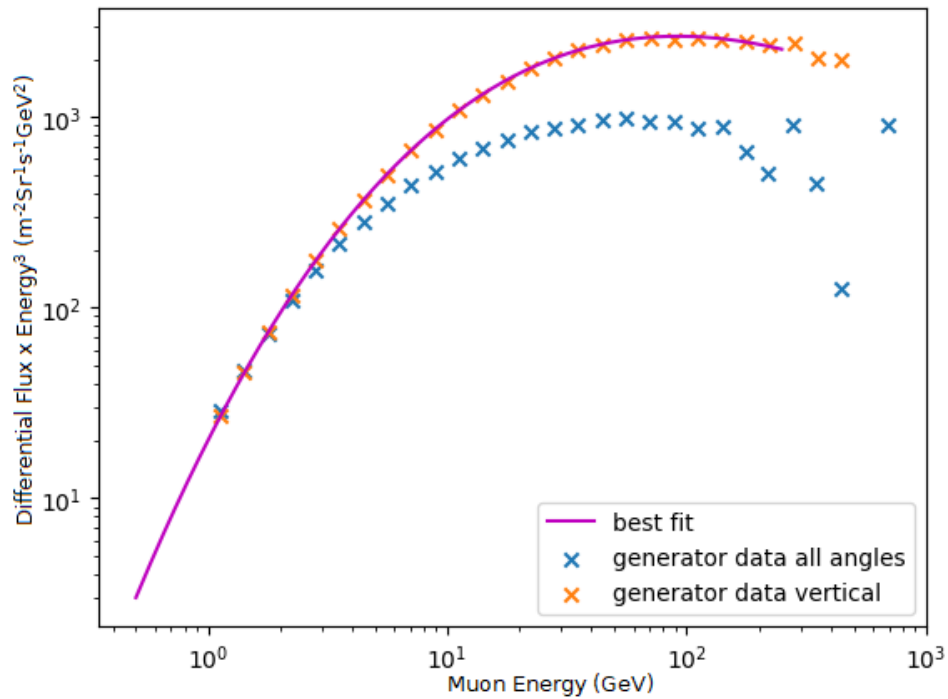


Figure 8: A plot of the generator output compared to best fit line after the bug in the rejection sampling algorithm has been fixed. The generator now accurately reproduces the best fit line for the vertical case. No further changes were needed for the 'vertical only' mode although the functionality was slightly altered so it could be used as part of the 'all angles' mode.

3.5 Time generation

For each of the two generation modes, times can also be generated. The generator is initially normalized to produce an overall flux of $70s^{-1}Sr^{-1}m^{-2}$ [6]. However, as this flux only includes muons above $1GeV$, the generator currently overestimates the arrival time of the muons. The times are generated from an exponential distribution with the rate calculated from the overall flux and detector area. The distribution of the arrival times follows an approximately uniform distribution as expected.

It is important to note, however, that data regarding the actual arrival times of muons is not available beyond the overall flux so any irregularities in the muon arrival rate cannot be accurately modelled. For the purposes of the generator, the arrival rate is simply assumed to be uniform.

3.6 Goals for the generator

Following the validation steps described above, the following goals were set;

- The angular spectrum produced should be accurate for higher energies. It is clear that the $\cos^2\theta$ distribution is not able to produce this spectrum. However, it is expected that with the more accurate angular spectrum, the $\cos^2\theta$ relation should still be preserved at low energies.
- The generator should be self-consistent. The generator output for vertical muons depends on which generation mode is used. As the 'correct' distribution is available, both generation modes should be able to produce it.
- The generator should be easy to install and use. Currently, the generator requires the user to read through the code to find the correct function and class to call for generation. This should be changed and clear instructions for installation and usage should be written.

4 Generator corrections

4.1 Vertical only mode

For this generation mode, the method of generation was not changed. The generator initially had a bug where the wrong curve would be selected at certain points leading to the erroneous distribution shown in figure 4. This was fixed and the vertical generation mode now agrees with experimental data.

4.2 All angles mode

Tests from section 3.3 showed that the $\cos^2\theta$ curve used to generate angles was unsuitable. However, due to the way the generator is programmed initially, an overall angular distribution was needed.

The generator first picks out an angle from the $\cos^2\theta$ distribution and then for each angle, the theoretical model (equation 1) at angle θ was used as the probability distribution for the rejection sampler to generate the corresponding energy.

An attempt to characterize the angular distribution involved using CORSIKA[17], an air shower simulation program. If the exponent of the $\cos^n\theta$ distribution is known for each cutoff energy, the angular distribution can be generated accurately. Runs of CORSIKA were done assuming that primary cosmic rays are isotropic and range from angles $\theta = 0^\circ$ to $\theta = 70^\circ$, the maximum range allowed in CORSIKA. The simulation was done in two separate runs, one using protons as the primaries and the other using helium nuclei. For each run, 20000 air showers were simulated. The results are shown in figure 9.

Despite many attempts at running the simulation, the $\cos^n\theta$ spectrum was unable to be recreated. This is most likely due to an insufficient number of showers despite making simplifying assumptions like assuming translation invariance.

The current iteration of the generator uses a different method to avoid needing to characterize the exponent. Since the energy distribution for vertical muons is very well known, using this data in the generator seemed much more attractive than using the angular spectrum.

Since the angular spectrum from equation 1 was found to be accurate, an overall energy distribution for muons of all zenith angles can be obtained by integrating over all angles at every energy in the best fit line. The generator would then be able to generate an energy from this curve.

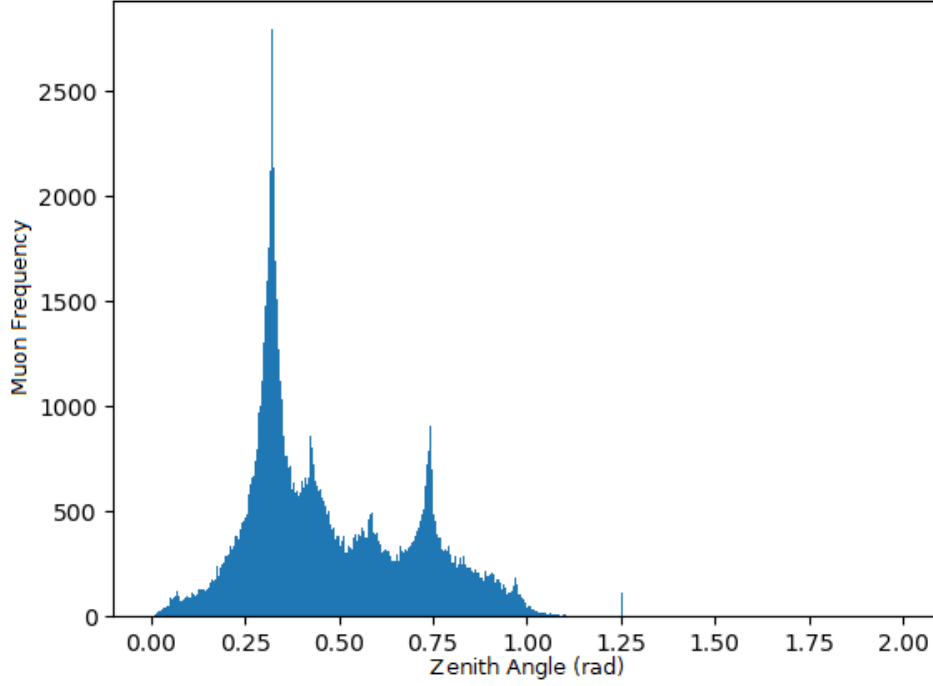


Figure 9: A plot of the frequency of muons against zenith angle as simulated in CORSIKA. This does not resemble the expected $\cos^2\theta$ distribution so this method of fitting the angular distribution was unsuitable. The plot also shows the limitations of CORSIKA with the maximum zenith angle allowed in the program being 70° ($\sim 1.22\text{rad}$).

Thus, the generator would be able to circumvent the energy limit problem described above by first selecting an energy from the overall energy curve which is between the user specified limits and then assigning an angle to each energy by computing equation 1 at each energy. However, there is no analytical solution to this integral so the integral was computed numerically using SciPy’s integrate library[19]. Figure 10 shows the experimental best fit compared to the estimated overall energy distribution (integrated over all angles). For the purposes of the generator, an order 6 polynomial was fitted to the integrated energy curve using NumPy’s polyfit function [20]. The fitting was very accurate with 1000000 points used for the fit and a residual of 3.07 and results using either curve match very well. This was necessary since computing the integral every time slowed the generator by ~ 50 times compared to computing the polynomial curve.

This method turns out to be very good at reproducing the angular spectrum even at higher energies and has the benefit of keeping the generator self-consistent when it comes to predicting the energy spectrum of near-vertical muons.

4.3 Time Generation

To generate time stamps for muons, the overall muon flux is required. The value of $70\text{s}^{-1}\text{Sr}^{-1}\text{m}^{-2}$ [6] is used for muons above 1GeV. The overall energy curve described in section 4.2 was used to estimate the muon flux at all energies by applying the appropriate scaling to the curve and integrating over a large energy range. This gave a total muon flux of $86.6\text{s}^{-1}\text{Sr}^{-1}\text{m}^{-2}$.

4.4 Ease of use

Following changes made to the generator, the generator was packaged into a command line program which can be built through pip. This allows for easy distribution and setup. Details on the installation are included in the Appendix.

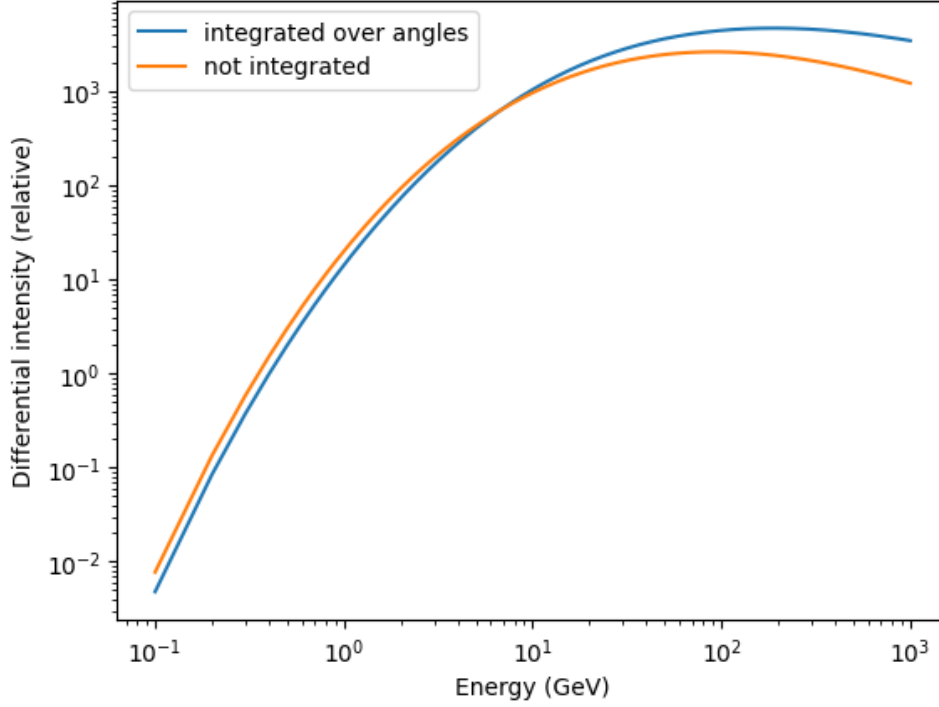


Figure 10: A plot of the energy distribution at $\theta = 0$ compared to the estimated energy distribution over all angles. Integrating over all angles has the effect of decreasing the amount of low energy muons compared to high energy ones. This result makes sense when considering the claim that at higher energies, the angular distribution follows a $\sec^n \theta$ distribution[18] This would mean that a lot of high energy muons are found at a larger zenith angle.

5 Validation of corrected generator

Following the corrections described in section 4, the generator was tested by comparing the output to various experiments done on the angular spectrum of sea-level muons. As before, the generator was set to generate 200000 muons using both settings.

5.1 Vertical muons

To validate the generator output, the results from the two generation modes were compared to the best fit line. For the 'all angles' mode, any muons with zenith angle below 2.5° were selected as vertical muon. The results are shown in figure 11.

5.2 Non-vertical muons

Experiments involving the angular spectrum of muons are often incompatible since the energy limits vary from experiment to experiment. Thus, data from each experiment was tested separately.

Throughout the testing, scaling between the differential flux of the generator and experiment was allowed since the absolute value of the differential flux only becomes relevant once the time generator has been implemented. Therefore, to claim that the generator is correct, it has to be able to produce the correct energy distribution at any angle and the correct angular distribution at any energy.

To prove that the generator can produce the correct spectrum for a wide range of energies and angles simultaneously, all subsequent tests except for the high energy one were done on data produced from one run of the generator with 200000 muons.

First, the angular spectrum at different energies was tested. The generator shows good agreement with the angular spectrum at two of the energies measured ($E_{mean} = 12.5$ and $22.5 GeV$) in [13]. However, the results at $E_{mean} = 45 GeV$ have a very large variance so it is difficult to make any claims regarding the agreement at this energy. The generator output was also compared to data obtained in [16] which

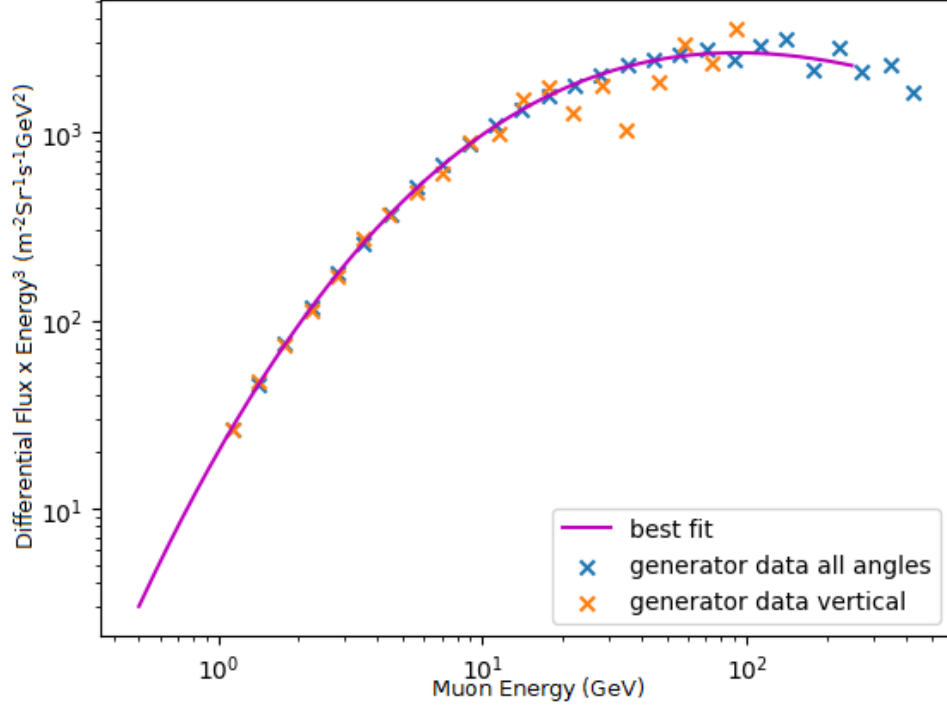


Figure 11: A plot of the generator output against the best fit line. The two generation modes now agree and both match the best fit line very well.

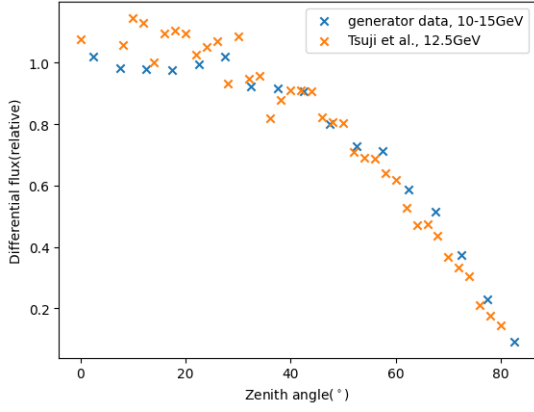
contains data for the $\theta = 55 - 85^\circ$. The generator is able to produce energy spectra at non-zenith angles which are consistent with the experimental data given.

When it comes to the energy spectrum at each angle, the generator is also able to recreate the experimental results. Figure 14 shows some of the data in [13] and [16] plotted against the generator output. The deviation at higher energy is most likely due to the lower muon flux resulting in more variance in the estimated differential intensity.

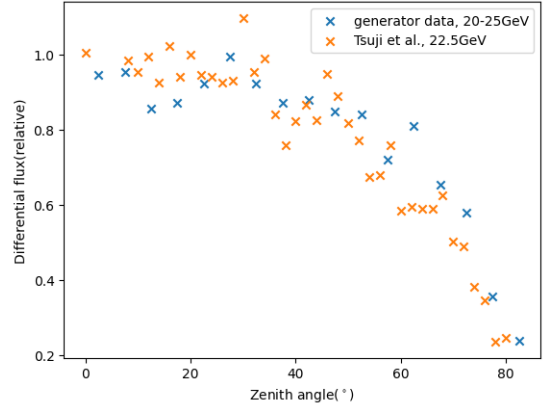
In addition to testing at specific energies, the integral flux was also tested as this is a well known relationship. For this test, the minimum energy cutoff was set to 0.5GeV and the results are binned in the same way as above. The resulting distribution was tested by performing a least square fit for a curve of type $\cos^n\theta$ with n as the fitting parameter. The curves were normalized such that the differential flux matches at $\theta = 0$. The resulting angular spectrum gives $n = 1.51$. Results in [8] report a value of $n = 1.72$ for a minimum energy cutoff of 0.6GeV . This test is particularly important since no reference was made to a $\cos^2\theta$ angular spectrum at any point in the generation method following the changes described in section 4.

The high energy limit of the generator was also tested. The integral spectrum for high energy muons is expected to follow a $\sec^n\theta$ distribution[18]. In [18], the exponents were measured at various energy cutoffs. These experiments were recreated using the generator and the results are shown in figure 16.

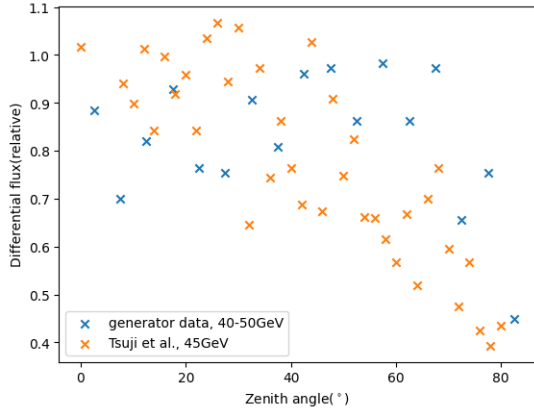
For the energy cutoff at 270GeV , the exponent was $n = 0.459$ which agreed with the exponent measured in [18] of 0.4 . For the cutoff at 540GeV , a least squares fit gave $n = 0.62$ which is slightly higher than the exponent given in the paper of 0.5 . Thus, the generator is able to recreate the high energy spectrum somewhat accurately. For this test, the generator was run again setting the lower limit to 200GeV . This was done because the initial run with the lower limit at 0GeV did not produce enough high energy muons to perform a meaningful test of the results in this energy range.



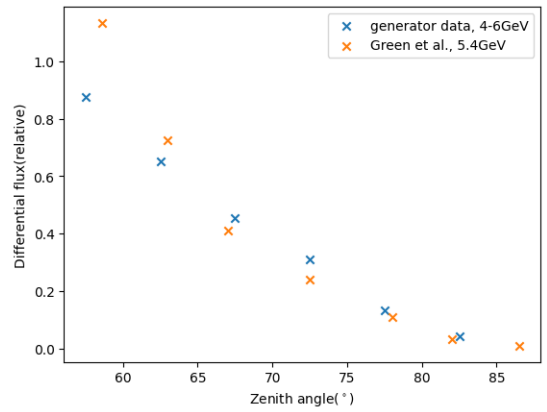
(a) 10 – 15 GeV



(b) 20 – 25 GeV

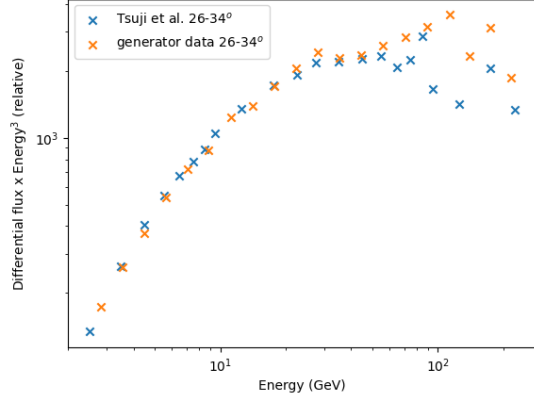


(c) 40 – 50 GeV

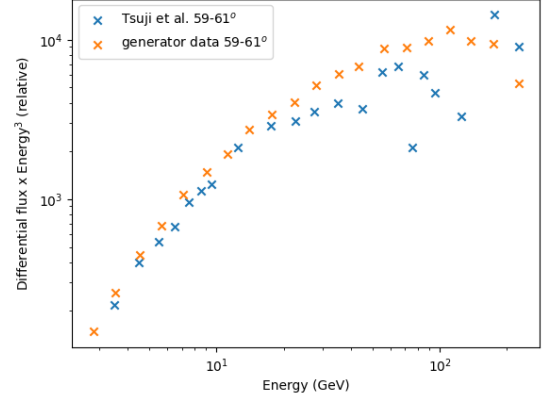


(d) 4 – 6 GeV

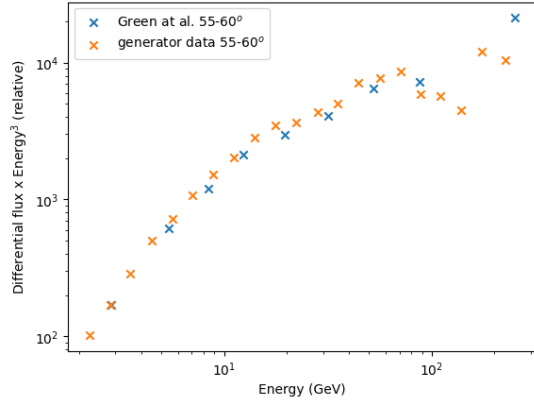
Figure 12: The generator output is seen to agree with experimental results very well in figures 12(a), 12(b) and 12(d). However, the distribution in 12(c) is very spread out. This is due to the smaller number of muons recorded in this energy range. In the paper presenting these results, the bins in this energy range contained significantly fewer muons than in other energy ranges (~ 10 times lower). The fact that the generator output also experienced a similar problem at a similar energy range is promising as it implies that the correct number of muons at each energy has been generated.



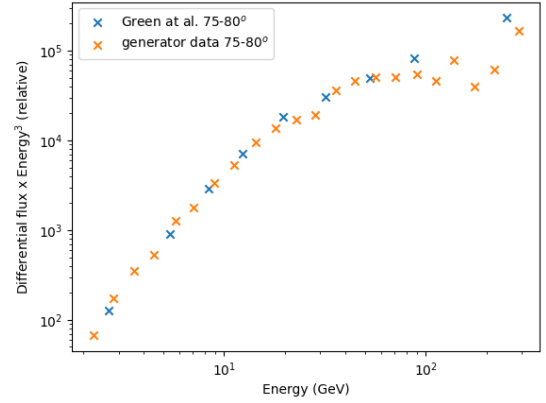
(a) $26 - 34^\circ$



(b) $59 - 61^\circ$



(c) $55 - 60^\circ$



(d) $75 - 80^\circ$

Figure 13: The generator output appears to agree with experimental results in the ranges given. Some deviations appear at higher energies although the lower muon count at those energies are most likely the reason why this deviation appears.

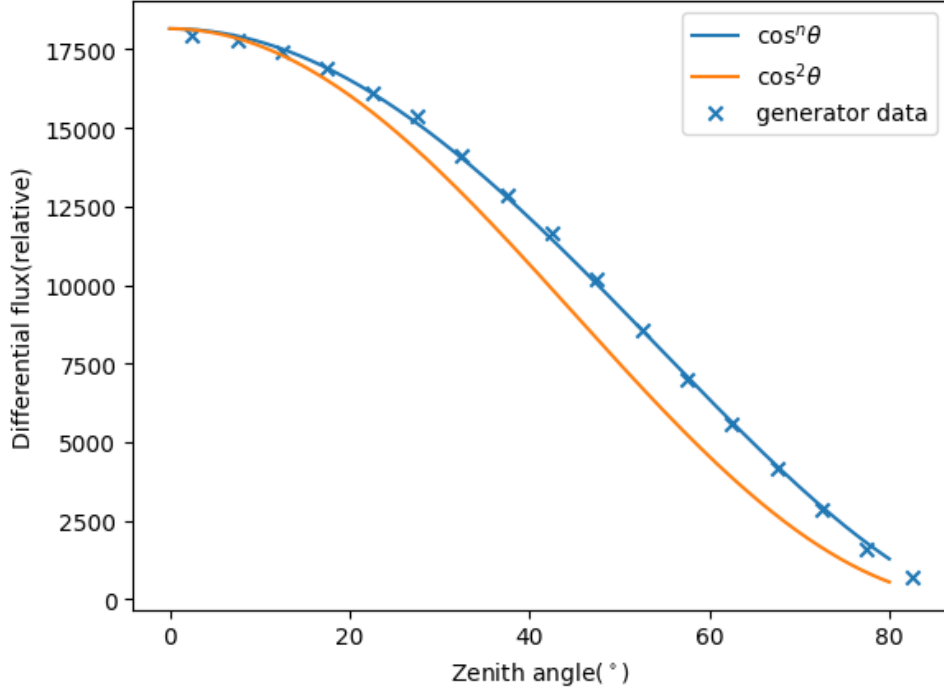
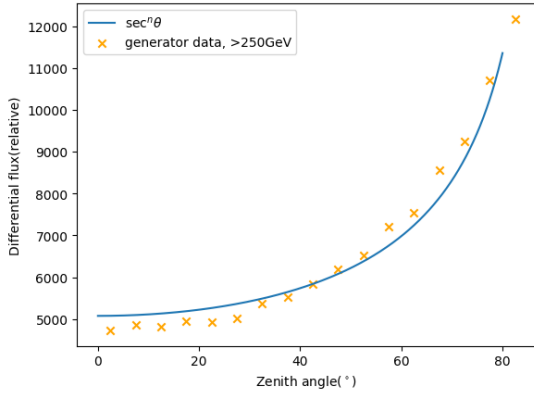
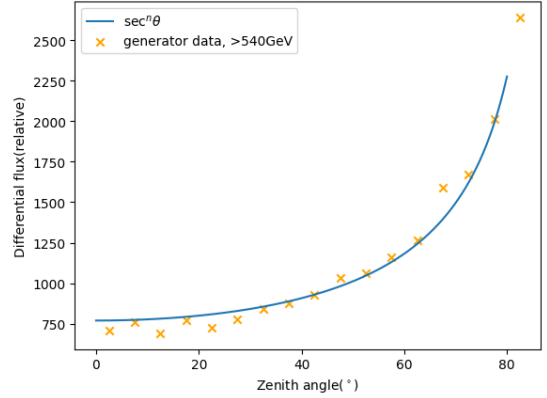


Figure 14: A plot of the generator output for all muons with energy more than 0.6GeV compared to a $\cos^n\theta$ and $\cos^2\theta$ plot. A least squares fit for the $\cos^n\theta$ curve gives $n = 1.51$ which is comparable to the experimental value of $n = 1.72$ in [8].



(a) $E > 250\text{GeV}$



(b) $E > 540\text{GeV}$

Figure 15: The generator output is able to predict the exponent n relatively accurately. The exponents are predicted to be 0.459 and 0.620 compared to experimental values of 0.5 and 0.6 at the minimum energies of 250 and 540GeV respectively.

6 Limitations

Possible sources of inaccuracies in the generator are highlighted in this section and the ranges where they might affect the output was estimated.

6.1 Theoretical Model

Since the angular dependence on the generator is entirely dependent on the theoretical parameterize, any assumptions made in the derivation also applies to the generator. Firstly, the derivation of equation 1 neglects any large curvatures in the earth's surface which means that for near-horizontal muons, the angular spectrum could be inaccurate[21]. The theoretical model is also inaccurate for low energy muons.

Although the problem is alleviated by the refitting described in section 4.2, there is no theoretical backing for this process. The generator does seem to produce the correct results so any errors should be relatively small. [21] suggests an alternative expression for the muon flux however this was not incorporated into the generator due to time constraints preventing proper testing of this parameterization. Any effects due to this factor would affect muons with energy $< 100\text{GeV}$ and zenith angles $> 70^\circ$.

6.2 Positive vs negative muons

Throughout the creation of the generator, the muon flux was assumed to be invariant to changes in the azimuthal angle. However, this is not correct. Many experiments have recorded the east-west effect responsible for the asymmetry in the muon flux [22][12]. The primary cause of this is thought to be the difference in the effect of Earth’s magnetic field on positively charged and negatively charged muons which cause them to be deflected in opposite directions. This can be seen directly in figure 3 from the data recorded by the BESS spectrometer which have recorded the flux of positive and negative muons separately. This effect is only noticeable in muons with energy in the order of 1GeV . [22] recorded the asymmetry peaking at around $\theta = 20^\circ$ with a magnitude of $\sim 4-5\%$. Most experiments used to generate the best fit line did not take into account any differences between the oppositely charged muons so it effectively forms an average flux of the two types of muons.

6.3 Lack of experimental data

Experimental data regarding the energy spectrum of muons at very high energy is lacking. Data from Ivanenko et al. [23] was the highest energy data set used. The maximum energy was $\sim 20\text{TeV}$. Although the generator is allowed to operate beyond this energy, it is important to note that above this energy, no testing has been done. It is expected that equation 1 describes the muon distribution at high energies very well due to the lower interaction time with the atmosphere so no limit has been put on the generator.

Data for near-horizontal muons is also lacking. [22] suggests that the theoretical model used is expected to accurately predict the angular spectrum up to $\sim 70^\circ$. Testing of the generator itself suggests that the angular spectrum is still accurate up to $\sim 80^\circ$. However, the accuracy beyond this range is unknown.

7 Conclusion

The cosmic ray event generator developed in [1] was tested and corrections were made to improve the accuracy of the generator. The generator now agrees with many of the experiments done in this field and is able to recreate the angular spectrum relatively accurately at all energies tested. It is also able to predict the $\cos^n\theta$ relation often quoted in literature without making any reference to this in its creation. The generator was then packaged in a way that is easy to distribute and run. All the goals set out in section 3.6 were accomplished.

A Installation and setup

The code for the generator and notebooks used to create the plots in this paper is available at github.com/someone-random/cosmic_ray_generator.git. The generator can be built using pip and run as a command line program. Instructions for installation are available at the github link above. The generator source code is located in the /api folder and the notebooks for generating the plots are in the /utility folder.

References

- [1] Sam Reynolds. “Building an effective sea-level cosmic ray generator”. In: (2022). URL: <https://www.hep.phy.cam.ac.uk/~lester/teaching/PartIIIProjects/2022-SamReynolds-report.pdf>.
- [2] “Atmospheric muons and neutrinos”. In: *Cosmic Rays and Particle Physics*. Cambridge University Press, June 2016, pp. 126–148. DOI: [10.1017/cbo9781139192194.008](https://doi.org/10.1017/cbo9781139192194.008). URL: <https://doi.org/10.1017/cbo9781139192194.008>.

- [3] L. F. Thompson et al. “Muon tomography for railway tunnel imaging”. In: *Physical Review Research* 2.2 (Apr. 2020). DOI: [10.1103/physrevresearch.2.023017](https://doi.org/10.1103/physrevresearch.2.023017). URL: <https://doi.org/10.1103/physrevresearch.2.023017>.
- [4] Haruo Miyadera et al. “Imaging Fukushima Daiichi reactors with muons”. In: *AIP Advances* 3.5 (May 2013), p. 052133. DOI: [10.1063/1.4808210](https://doi.org/10.1063/1.4808210). URL: <https://doi.org/10.1063/1.4808210>.
- [5] Kunihiro Morishima et al. “Discovery of a big void in Khufu’s Pyramid by observation of cosmic-ray muons”. In: *Nature* 552.7685 (Nov. 2017), pp. 386–390. DOI: [10.1038/nature24647](https://doi.org/10.1038/nature24647). URL: <https://doi.org/10.1038/nature24647>.
- [6] M. Tanabashi et al. “Review of Particle Physics”. In: *Physical Review D* 98.3 (Aug. 2018). DOI: [10.1103/physrevd.98.030001](https://doi.org/10.1103/physrevd.98.030001). URL: <https://doi.org/10.1103/physrevd.98.030001>.
- [7] Hariom Sogarwal and Prashant Shukla. “Measurement of atmospheric muon angular distribution using a portable setup of liquid scintillator bars”. In: *Journal of Cosmology and Astroparticle Physics* 2022.07 (July 2022), p. 011. DOI: [10.1088/1475-7516/2022/07/011](https://doi.org/10.1088/1475-7516/2022/07/011). URL: <https://doi.org/10.1088/1475-7516/2022/07/011>.
- [8] Issa Briki, Malek Mazouz, and Lotfi Ghedira. “Angular distribution of low momentum atmospheric muons at ground level”. In: (2022). DOI: [10.1088/1475-7516/2023/04/025](https://doi.org/10.1088/1475-7516/2023/04/025). eprint: [arXiv: 2206.13061](https://arxiv.org/abs/2206.13061).
- [9] M. Bahmanabadi. “A method for determining the angular distribution of atmospheric muons using a cosmic ray telescope”. In: *Nuclear Instruments and Methods in Physics Research Section A: Accelerators, Spectrometers, Detectors and Associated Equipment* 916 (Feb. 2019), pp. 1–7. DOI: [10.1016/j.nima.2018.11.010](https://doi.org/10.1016/j.nima.2018.11.010). URL: <https://doi.org/10.1016/j.nima.2018.11.010>.
- [10] R. R. S. de Mendonça et al. “THE TEMPERATURE EFFECT IN SECONDARY COSMIC RAYS (MUONS) OBSERVED AT THE GROUND: ANALYSIS OF THE GLOBAL MUON DETECTOR NETWORK DATA”. In: *The Astrophysical Journal* 830.2 (Oct. 2016), p. 88. DOI: [10.3847/0004-637x/830/2/88](https://doi.org/10.3847/0004-637x/830/2/88). URL: <https://doi.org/10.3847/0004-637x/830/2/88>.
- [11] George Casella, Christian P. Robert, and Martin T. Wells. “Generalized Accept-Reject sampling schemes”. In: *Institute of Mathematical Statistics Lecture Notes - Monograph Series*. Institute of Mathematical Statistics, 2004, pp. 342–347. DOI: [10.1214/lnms/1196285403](https://doi.org/10.1214/lnms/1196285403). URL: <https://doi.org/10.1214/lnms/1196285403>.
- [12] M Motoki et al. “Precise measurements of atmospheric muon fluxes with the BESS spectrometer”. In: *Astroparticle Physics* 19.1 (Apr. 2003), pp. 113–126. DOI: [10.1016/s0927-6505\(02\)00195-0](https://doi.org/10.1016/s0927-6505(02)00195-0). URL: [https://doi.org/10.1016/s0927-6505\(02\)00195-0](https://doi.org/10.1016/s0927-6505(02)00195-0).
- [13] Shuhei Tsuji et al. “Measurements of muons at sea level”. In: *Journal of Physics G: Nuclear and Particle Physics* 24.9 (Sept. 1998), pp. 1805–1822. DOI: [10.1088/0954-3899/24/9/013](https://doi.org/10.1088/0954-3899/24/9/013). URL: <https://doi.org/10.1088/0954-3899/24/9/013>.
- [14] O.C. Allkofer, K. Carstensen, and W.D. Dau. “The absolute cosmic ray muon spectrum at sea level”. In: *Physics Letters B* 36.4 (Sept. 1971), pp. 425–427. DOI: [10.1016/0370-2693\(71\)90741-6](https://doi.org/10.1016/0370-2693(71)90741-6). URL: [https://doi.org/10.1016/0370-2693\(71\)90741-6](https://doi.org/10.1016/0370-2693(71)90741-6).
- [15] C A Ayre et al. “Precise measurement of the vertical muon spectrum in the range 20-500 GeV/c”. In: *Journal of Physics G: Nuclear Physics* 1.5 (June 1975), pp. 584–600. DOI: [10.1088/0305-4616/1/5/010](https://doi.org/10.1088/0305-4616/1/5/010). URL: <https://doi.org/10.1088/0305-4616/1/5/010>.
- [16] P. J. Green et al. “Absolute intensities of medium-energy muons in the vertical and at zenith angles 55°–85°”. In: *Physical Review D* 20.7 (Oct. 1979), pp. 1598–1607. DOI: [10.1103/physrevd.20.1598](https://doi.org/10.1103/physrevd.20.1598). URL: <https://doi.org/10.1103/physrevd.20.1598>.
- [17] D. Heck et al. *CORSIKA: a Monte Carlo code to simulate extensive air showers*. 1998.
- [18] V. V. Borog et al. “Study of angular distribution of high-energy cosmic ray muons at large zenith angles”. In: *International Cosmic Ray Conference*. Vol. 4. International Cosmic Ray Conference. Jan. 1970, p. 179.
- [19] Pauli Virtanen et al. “SciPy 1.0: Fundamental Algorithms for Scientific Computing in Python”. In: *Nature Methods* 17 (2020), pp. 261–272. DOI: [10.1038/s41592-019-0686-2](https://doi.org/10.1038/s41592-019-0686-2).
- [20] Charles R. Harris et al. “Array programming with NumPy”. In: *Nature* 585.7825 (Sept. 2020), pp. 357–362. DOI: [10.1038/s41586-020-2649-2](https://doi.org/10.1038/s41586-020-2649-2). URL: <https://doi.org/10.1038/s41586-020-2649-2>.

- [21] Prashant Shukla and Sundaresh Sankrith. *Energy and angular distributions of atmospheric muons at the Earth*. 2016. eprint: [arXiv:1606.06907](https://arxiv.org/abs/1606.06907).
- [22] S Abdollahi, M Bahmanabadi, and D Purmohammad. “Study of atmospheric muons using a cosmic ray telescope”. In: *Journal of Physics G: Nuclear and Particle Physics* 40.2 (Jan. 2013), p. 025202. DOI: [10.1088/0954-3899/40/2/025202](https://doi.org/10.1088/0954-3899/40/2/025202). URL: <https://doi.org/10.1088/0954-3899/40/2/025202>.
- [23] I. Ivanenko et al. “Results of investigation of muon fluxes of superhigh energy cosmic rays with X-ray emulsion chambers”. In: (Sept. 1985).